Beam-Selection Performance Analysis of a Switched Multibeam Antenna System in Mobile Communications Environments

Tadashi Matsumoto, *Senior Member, IEEE,* Seiji Nishioka, *Member, IEEE,* and David J. Hodder, *Member, IEEE*

***Abstract*—The probability of incorrect beam selection (PIBS) with a switched multibeam antenna system is theoretically analyzed under power-limited and interference-limited mobile communication environments. Periodic transmission of unique word sequence followed by information symbol sequence is assumed. The model of beam selection used in this paper is based upon a simple three-stage mechanism: 1) signal validation; 2) averaging; and 3) selection of the largest output. Complex correlation peaks corresponding to the unique words, detected by the matched filter for the signal validation, are averaged over several consecutive unique words, and a beam having the largest output is selected. Equally weighted noncoherent integration is assumed for the averaging process. The beam selection takes place frame-by-frame.**

The first half of this paper is devoted to the PIBS derivation for a simple switched two-beam antenna system. Numerical calculation results are then presented. The latter half of this paper investigates the impact of the incorrect beam selection on overall average signal-to-noise (SNR) power ratio and signal-to-interference (SIR) power ratio. The amount of the overall SNR (or SIR) improvement over the omnidirectional antenna depends on the propagation conditions. In general, larger improvements can be achieved by smaller values of PIBS.

***Index Terms*—Digital cellular system, switched multibeam antenna, TDMA, time diversity, unique word detection.**

I. Introduction

THE ARRAY antenna with adaptive beam forming has been recognized as being effective in suppressing cochannel interference by steering nulls to interferers, thereby improving the signal-to-interference (SIR) power ratio on the desired signal component. In cellular configurations, this allows cochannel interferers to be located in cells closer to the reference cell than those with omnidirectional antennas, or even in the same cell. References [1] and [2] analyze the capacity enhancement achieved by a base-station array antenna system with adaptive beam forming and discuss a practical antenna configuration. Reference [3] analyzes the capacity improvement with a base-station antenna array for a code division multiple access (CDMA) mobile communications system.

One major drawback of the adaptive beam-forming array antenna is that given the number of array elements, the beam gains are subject to the users' geographical locations: the shorter the geographical distance between the desired user and interferers, the smaller the beam gain. This problem can be eliminated by adaptive signal *combining* [4]–[6] rather than beam *forming*. The array antenna system with adaptive signal combining does not require the antenna elements to be located close enough to achieve beam directivity, but it requires them to be separated in space so that fading variations on the received signals can be regarded as statistically independent. This requirement is similar to diversity reception. Reference [7] derives, given a number of antenna elements, the number of interferers the array can suppress and the equivalent diversity order the array achieves. With this idea, several users' signals, even coming from the same direction, can be resolved.

Both the beam-forming and signal combining antennas require adaptive signal processing to determine the optimal weight coefficients that meet their criteria. In mobile communications environments, the received complex envelopes of the desired and interference signals vary rapidly due to fading. Therefore, the adaptive signal processing must "track" the change in the fading envelope so that the weight coefficients *always* meet the optimality requirements. If the tracking performance with the adaptive algorithm is not sufficient, antenna performances may degrade.

One simple alternative to the adaptive antennas is the switched multibeam antenna system, in which several narrow beams are used to cover the entire coverage of the base station [8]. A beam receiving the desired signal with the highest signal strength among the beams is selected. Even with this simple mechanism, the spectrum efficiency of the cellular system can be improved. This is because the narrower the beam, the smaller the probability that interference signals are received by the same beam selected for the desired signal. A similarity may be found between this concept and sectored cell configurations. However, the switched beam antenna does not require a handoff process, even if a user moves to another beam. Handoff to a *different carrier* may be initiated if none of the signals received by any beams does not satisfy a quality requirement.

Manuscript received April 21, 1995; revised October 11, 1995 and February 28, 1996.

T. Matsumoto was with NTT America, Inc., Lafayette, CA 94549 USA. He is now with NTT Mobile Communications Network, Inc., Yokosuka, Kanagawa 239, Japan.

S. Nishioka was with NTT America, Inc., Lafayette, CA 94549 USA. He is now with NTT America, New York, NY 10178 USA.

D. Hodder is with Telecommunications Group, Inc., Houston, TX 77004 USA.

Publisher Item Identifier S 0018-9545(97)01308-X.

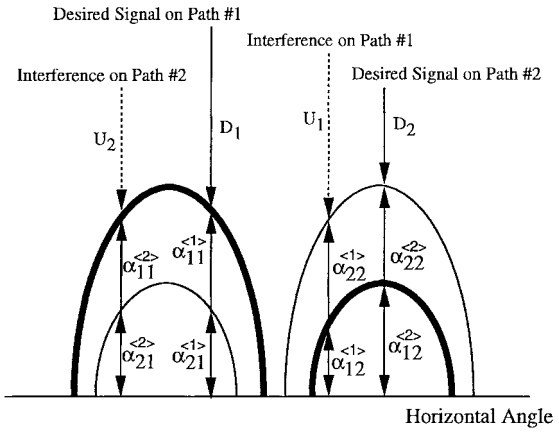

Fig. 1. Propagation scenario and antenna gains.

The beam selection takes place using a sequence of unique words periodically embedded in the transmitted symbol sequence, and the sequence received by the selected beam is output. Each antenna element is followed by a filter matched to the unique word waveform. Simple signal processing using the outputs of the matched filters suppresses the effect of interferences on the beam selection. This process is referred to as "validation" for convenience. However, this signal validation process may not be perfect. Hence, a major problem inherent within the switched multibeam antenna system is incorrect beam selection; a beam receiving a desired signal component having the highest SIR *plus* noise power ratio cannot be selected. Therefore, a pragmatic consideration should be given to two issues: how frequently the incorrect beam selection happens under various mobile propagation scenarios and how serious the outcome is that results from the incorrect selection.

This paper theoretically analyzes the probability of incorrect beam selection (PIBS) with a switched multibeam antenna system. A two-beam antenna is assumed for simplicity. It is assumed that there is one desired user and one interferer and that each of the desired and interference transmissions has two propagation paths: one goes to one of the two beams and the other goes to the other beam. It is shown that the PIBS is dominated by the power ratio of the two desired signal components; if the ratio is small, a relatively high PIBS results.

The impact of the incorrect beam selection on overall average signal-to-noise power ratio (SNR) and SIR power ratio is then investigated. It is shown that in both the power-limited and interference-limited environments, larger overall SNR (or SIR) improvements over the omnidirectional antenna can be achieved with smaller values of the average PIBS. The amount of the improvement depends on the power ratios of both the two desired signal components and two interference signal components.

This paper is organized as follows. Section II presents the system model used. A mathematical model of the signal processing for the signal validation and beam selection is described. In Section III, it is shown that the decision variable used in the beam-selection process can be expressed as a quadratic form of the complex random variable vector comprised of desired, interference, and noise components at the matched filter output. This implies that eigenvalues of the matrix with the quadratic form are needed to calculate the PIBS. Some numerical algorithms may be applicable to the eigen analysis. Section IV presents, for the quaternary phase shift keying (QPSK), numerical calculation results for the PIBS under various propagation environments. In Section V, the impacts of the incorrect beam selection on the overall SNR and SIR enhancements are discussed.

II. System Model

A. Channel Model

There is one desired user and one cochannel interferer in the system being considered. The base station has a switched two-beam antenna system. Each antenna's main beam covers a separate area, but its side lobe overlaps another main beam's coverage.[1] Each of the desired and interference transmissions has two propagation paths: one goes to one of the two element's main beams and the other goes to the other. As shown in Fig. 1, main beams and their side lobes have complex beam gains of $\alpha_{ij}^{\langle p \rangle}$, where i and j each take values of one or two. i indexes the antenna element, j expresses the direction of the ith element's main beam, and $\langle p \rangle$ expresses each user's pth propagation path.

It is assumed that the two propagation paths for each user are subjected to independent frequency-flat Rayleigh fading. Fading variation with the desired signal is statistically independent of that with the interference. A block diagram of the multipath channel and antenna system is shown in Fig. 2. Output samples $z_{rk}^{\langle 1 \rangle}$ and $z_{rk}^{\langle 2 \rangle}$ of the first and second elements can, respectively, be expressed as

$$\begin{aligned} z_{rk}^{\langle 1 \rangle} = {} & \alpha_{11}^{\langle 1 \rangle} z_{dk}^{\langle 1 \rangle} s_k + \alpha_{12}^{\langle 1 \rangle} z_{uk}^{\langle 1 \rangle} u_k + \alpha_{11}^{\langle 2 \rangle} z_{uk}^{\langle 2 \rangle} u_k \\ & + \alpha_{12}^{\langle 2 \rangle} z_{dk}^{\langle 2 \rangle} s_k + z_{nk}^{\langle 1 \rangle} \end{aligned} \tag{1.1}$$

and

$$\begin{aligned} z_{rk}^{\langle 2 \rangle} = {} & \alpha_{21}^{\langle 1 \rangle} z_{dk}^{\langle 1 \rangle} s_k + \alpha_{22}^{\langle 1 \rangle} z_{uk}^{\langle 1 \rangle} u_k + \alpha_{21}^{\langle 2 \rangle} z_{uk}^{\langle 2 \rangle} u_k \\ & + \alpha_{22}^{\langle 2 \rangle} z_{dk}^{\langle 2 \rangle} s_k + z_{nk}^{\langle 2 \rangle} \end{aligned} \tag{1.2}$$

where $z_{dk}^{\langle 1 \rangle} = z_d^{\langle 1 \rangle}(kT_s)$, $z_{dk}^{\langle 2 \rangle} = z_d^{\langle 2 \rangle}(kT_s)$, with $z_d^{\langle 1 \rangle}(t)$ and $z_d^{\langle 2 \rangle}(t)$ being, respectively, the fading complex envelopes with the desired user's first and second paths, $z_{uk}^{\langle 1 \rangle} = z_u^{\langle 1 \rangle}(kT_s)$, $z_{uk}^{\langle 2 \rangle} = z_u^{\langle 2 \rangle}(kT_s)$, with $z_u^{\langle 1 \rangle}(t)$ and $z_u^{\langle 2 \rangle}(t)$ being, respectively, the fading complex envelopes with the interferer's first and second paths, and T_s is the sampling period. $s_k = s(kT_s)$ and $u_k = u(kT_s)$, with $s(t)$ and $u_k = u(t)$ being, respectively, the desired user's and interferer's waveforms at the receiver filter output. We assume that the difference in the propagation delay between the two propagation paths is small enough compared to the sampling period T_s. $z_{nk}^{\langle 1 \rangle} = z_n^{\langle 1 \rangle}(kT_s)$ and $z_{nk}^{\langle 2 \rangle} = z_n^{\langle 2 \rangle}(kT_s)$, with $z_n^{\langle 1 \rangle}(t)$ and $z_n^{\langle 2 \rangle}(t)$ being, respectively, the filtered Gaussian noise components on the two antenna element outputs.

[1] The beam pattern itself is not within the scope of this paper; the two-beam configuration assumed in this paper is the model for the PIBS analysis. In actual base stations, antenna beams may have more complex patterns; even main beams may overlap each other. The PIBS derivation process described in this paper can be applied to that situation and should result in similarity in the performances.

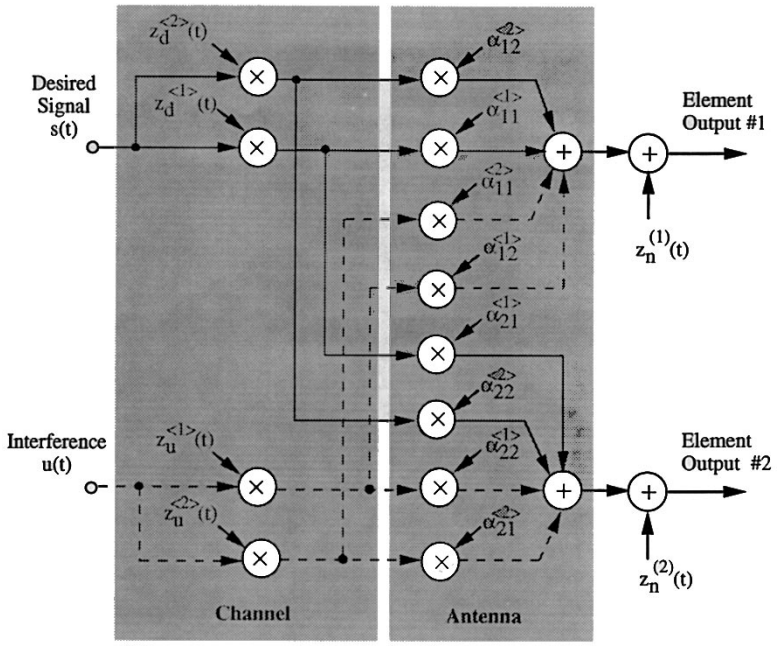

Fig. 2. Block diagram of multipath channel and antenna system.

B. Beam Selection

A block diagram for overall signal processing for the beam selection is shown in Fig. 3(a). The overall signal processing is comprised of three stages: 1) signal validation; 2) averaging; and 3) selection of the largest output. The signal validation process uses a sequence of unique words periodically embedded in the transmitted symbol sequence.[2] Fig. 3(b) shows the frame format. The symbol sequence received by the selected beam is output frame-by-frame. The unique word consists of L symbols. Sampling of the receiver filter output takes place M times a symbol. Hence, $T/T_s = M$, where T is the symbol duration.

Each antenna element is followed by a matched filter matched to the unique word waveform. A simple configuration of the matched filter is shown in Fig. 3(c). The sample sequence is the input to the matched filter. It is assumed that the receiver knows the timing at which the desired signal's unique word is received, but it does not know the interferer's transmitted symbol sequence. The interferer's symbol timing is asynchronous with the desired signal's symbol timing.

The matched filter output at that timing can be expressed as

$$\mathbf{z}^{(i)} = \mathbf{z}_r^{(i)}\mathbf{s}^{t*} \tag{2.1}$$

where

$$\mathbf{z}_r^{(i)} = [z_{r1}^{(i)} \quad z_{r2}^{(i)} \quad \cdots \quad z_{rLM}^{(i)}] \tag{2.2}$$

$$\mathbf{s} = [s_1 \quad s_2 \quad \cdots \quad s_{LM}] \tag{2.3}$$

$i = 1 \cdots 2$ indexes the element number, and t and $*$ denote transpose and complex conjugate, respectively. The matched filter output for the two antenna elements can be obtained by substituting (1.1) and (1.2) into (2.1). For the lth unique word, the matched filter outputs become

$$\begin{aligned} z_l^{(1)} = {} & \alpha_{11}^{\langle 1\rangle} z_{md}^{\langle 1\rangle} + \alpha_{12}^{\langle 1\rangle} z_{mu}^{\langle 1\rangle} + \alpha_{11}^{\langle 2\rangle} z_{mu}^{\langle 2\rangle} \\ & + \alpha_{12}^{\langle 2\rangle} z_{md}^{\langle 2\rangle} + z_{mn}^{(1)} \end{aligned} \tag{3.1}$$

and

$$\begin{aligned} z_l^{(2)} = {} & \alpha_{21}^{\langle 1\rangle} z_{md}^{\langle 1\rangle} + \alpha_{22}^{\langle 1\rangle} z_{mu}^{\langle 1\rangle} + \alpha_{21}^{\langle 2\rangle} z_{mu}^{\langle 2\rangle} \\ & + \alpha_{22}^{\langle 2\rangle} z_{md}^{\langle 2\rangle} + z_{mn}^{(2)} \end{aligned} \tag{3.2}$$

where

$$z_{md}^{\langle p\rangle} = \mathbf{z}_d^{\langle p\rangle}\mathbf{r}_{ss}^t \tag{3.3}$$

$$z_{mu}^{\langle p\rangle} = \mathbf{z}_u^{\langle p\rangle}\mathbf{r}_{su}^t \tag{3.4}$$

and

$$\mathbf{z}_{mn}^{(i)} = \mathbf{z}_n^{(i)}\mathbf{r}_s^t \tag{3.5}$$

with

$$\mathbf{z}_d^{\langle p\rangle} = [z_{d1}^{\langle p\rangle} \quad z_{d2}^{\langle p\rangle} \quad \cdots \quad z_{dLM}^{\langle p\rangle}] \tag{3.6}$$

$$\mathbf{z}_u^{\langle p\rangle} = [z_{u1}^{\langle p\rangle} \quad z_{u2}^{\langle p\rangle} \quad \cdots \quad z_{uLM}^{\langle p\rangle}] \tag{3.7}$$

$$\mathbf{z}_n^{\langle i\rangle} = [z_{n1}^{(i)} \quad z_{n2}^{(i)} \quad \cdots \quad z_{nLM}^{(i)}] \tag{3.8}$$

$$\mathbf{r}_{ss} = [s_1 s_1^* \quad s_2 s_2^* \quad \cdots \quad s_{LM} s_{LM}^*] \tag{3.9}$$

$$\mathbf{r}_{su} = [u_1 s_1^* \quad u_2 s_2^* \quad \cdots \quad u_{LM} s_{LM}^*] \tag{3.10}$$

$$\mathbf{r}_s = [s_1^* \quad s_2^* \quad \cdots \quad s_{LM}^*] \tag{3.11}$$

$i = 1 \cdots 2$, and $p = 1 \cdots 2$.

The best performance should be achieved by the coherent integration that first cophases the matched filter outputs and then sums them up. This process requires estimates of the complex fading envelope, for which some adaptive algorithms may be used. This is beyond the scope of this paper. One simple alternative to the averaging process in fading channels is noncoherent integration: the squared matched filter output

[2] Periodic unique word transmission is a popular technique in digital mobile communications systems. The unique word is usually used for many purposes such as radio link control, timing adjustment, quality checking, and equalization.

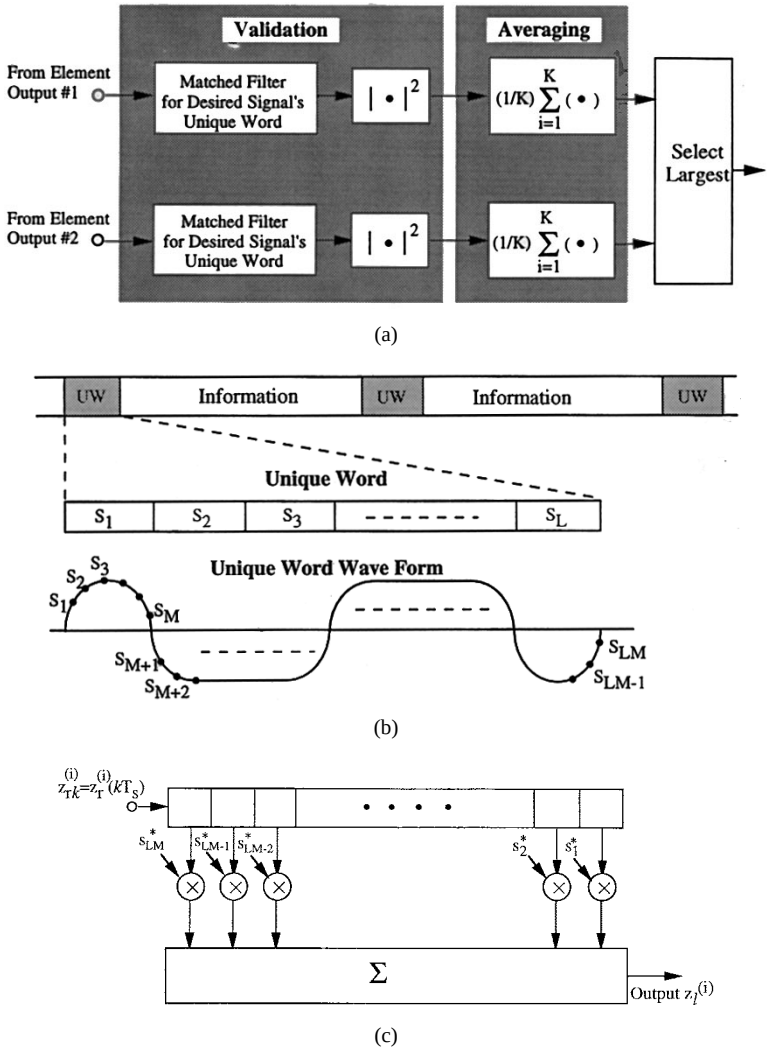

Fig. 3. (a) Block diagram for overall signal processing for beam selection, (b) frame format, and (c) matched filter for the unique word waveform.

$z_l^{(i)} z_l^{(i)*}$ is equally weighted and summed up[3] over several consecutive unique words. The noncoherent combiner output $D^{(i)}$ can then be expressed as

$$D^{(i)} = \sum_{l=1}^{K} z_l^{(i)} z_l^{(i)*} \tag{4}$$

where K is the averaging times. The decision on the beam selection is made based on the decision variable given by

$$D = \frac{D^{(1)} - D^{(2)}}{2}. \tag{5}$$

If $D \geq 0$, the beam corresponding to the first element is selected. Otherwise, the second beam is selected.

III. PIBS Derivation

A. One-Shot Observation

For the derivation of the PIBS, a special case with $K = 1$ is first considered for simplicity. After several manipulations, the decision variable $D = \{z_1^{(1)} z_1^{(1)*} - z_1^{(2)} z_1^{(2)*}\}/2$ is found to be expressed as

$$D = \frac{\mathbf{z}\mathbf{R}\mathbf{z}^{t*}}{2} \tag{6.1}$$

where

$$\mathbf{z} = [z_{md}^{\langle 1 \rangle} \quad z_{mu}^{\langle 1 \rangle} \quad z_{md}^{\langle 2 \rangle} \quad z_{mu}^{\langle 2 \rangle} \quad z_{mn}^{(1)} \quad z_{mn}^{(2)}] \tag{6.2}$$

and

$$\mathbf{R} = \begin{bmatrix} \mathbf{R}_{11} & \mathbf{R}_{12} \\ \mathbf{R}_{12}^{t*} & \mathbf{R}_{22} \end{bmatrix} \tag{6.3}$$

as shown in (6.4)–(6.6) at the bottom of the page. Hence, it is found that the decision variable D can be expressed as a quadratic form of the complex random variable vector $\mathbf{z}$.

The desired signal and interference components $z_{md}^{\langle p \rangle}$ and $z_{mu}^{\langle p \rangle}$ ($p = 1 \cdots 2$) at the matched filter output in (6.2) are the sums of the fading complex envelopes, as shown in (3.3) and (3.4), respectively. Hence, $z_{md}^{\langle p \rangle}$ and $z_{mu}^{\langle p \rangle}$ become zero-mean independent complex Gaussian processes with variances of $\langle |z_{md}^{\langle p \rangle}|^2 \rangle = \mathbf{r}_{ss} \mathbf{R}_d^{\langle p \rangle} \mathbf{r}_{ss}^{t*}$ and $\langle |z_{mu}^{\langle p \rangle}|^2 \rangle = \mathbf{r}_{su} \mathbf{R}_u^{\langle p \rangle} \mathbf{r}_{su}^{t*}$, where $\mathbf{R}_d^{\langle p \rangle}$ and $\mathbf{R}_u^{\langle p \rangle}$ are, respectively, the correlation matrices of

[3]The signal validation and noncoherent integration process is analogous with the energy detection of the supervisory audio tone (SAT) used in the advanced mobile phone service (AMPS) system for cell identification [11].

the fading complex envelopes with the desired user's and interferer's pth paths. Let $\mathbf{R}_d^{\langle p\rangle}$ and $\mathbf{R}_u^{\langle p\rangle}$ be denoted by

$$\mathbf{R}_d^{\langle p\rangle} = 2\sigma_{dp}^2 \begin{bmatrix} \rho_{1,1} & \cdots & \rho_{1,LM} \\ \vdots & \ddots & \vdots \\ \rho_{LM,1} & \cdots & \rho_{LM,LM} \end{bmatrix} \tag{7.1}$$

and

$$\mathbf{R}_u^{\langle p\rangle} = 2\sigma_{up}^2 \begin{bmatrix} \mu_{1,1} & \cdots & \mu_{1,LM} \\ \vdots & \ddots & \vdots \\ \mu_{LM,1} & \cdots & \mu_{LM,LM} \end{bmatrix} \tag{7.2}$$

where for $k = 1 \cdots LM$, $\sigma_{dp}^2 = \frac{1}{2}\langle |z_{dk}^{\langle p\rangle}|^2\rangle = D_p$ and $\sigma_{up}^2 = \frac{1}{2}\langle |z_{uk}^{\langle p\rangle}|^2\rangle = U_p$, with D_p being the average desired signal power of the pth propagation path and U_p being the average interference power of the pth propagation path. If Jakes' fading model [9] is used, $\rho_{m,n} = J_0(2\pi f_{Dd}|m-n|T_s)$ and $\mu_{m,n} = J_0(2\pi f_{Du}|m-n|T_s)$, where f_{Dd} and f_{Du} are the maximum Doppler frequencies for the desired user and interferer, respectively, and $J_0(\bullet)$ is the zeroth-order Bessel function of the first kind.

The noise components $z_{mn}^{(i)}$'s at the matched filter output in (6.2) are the sums of the samples of the filtered Gaussian noise, as shown in (3.5). Hence, $z_{mn}^{(i)}$'s also become zero-mean independent complex Gaussian processes with variances of $\langle |z_{mn}^{(1)}|^2\rangle = \langle |z_{mn}^{(2)}|^2\rangle = \mathbf{r}_s \mathbf{R}_n \mathbf{r}_s^{t*}$, where $\mathbf{R}_n$ is the correlation matrix of the filtered Gaussian process. Let $\mathbf{R}_n$ be denoted by

$$\mathbf{R}_n = 2\sigma_n^2 \begin{bmatrix} \phi_{1,1} & \cdots & \phi_{1,LM} \\ \vdots & \ddots & \vdots \\ \phi_{LM,1} & \cdots & \phi_{LM,LM} \end{bmatrix} \tag{8}$$

where $\sigma_n^2 = \frac{1}{2}\langle |z_{nk}^{(1)}|^2\rangle = \frac{1}{2}\langle |z_{nk}^{(2)}|^2\rangle = N$, with N being the noise power. If the receiver filter has its transfer function of $H(f)$, then

$$\phi_{m,n} = \phi^{(|m-n|T_s)} \tag{9.1}$$

with $\phi(\tau)$ being the autocorrelation function of the filtered noise given by

$$\phi(\tau) = \int_{-\infty}^{\infty} |H(f)|^2 \exp\{j2\pi f\tau\}\, df. \tag{9.2}$$

Since (6.1) is a quadratic form of the complex random variable vector $\mathbf{z}$, the decision variable D's characteristic function $\varphi(s) = \langle e^{-sD}\rangle$ can be expressed using the matrix $\mathbf{R}$, given by (6.3) as

$$\varphi(s) = \frac{1}{\det(I + s\mathbf{R}^{t*}\mathbf{R}_{du})} \tag{10}$$

where $\mathbf{R}_{du}$ is $\mathbf{z}$'s autocorrelation matrix given by (11), as shown at the bottom of the page. The characteristic function given by (10) can be rewritten as

$$\varphi(s) = \prod_{m=1}^{6} \frac{1}{1+s\lambda_m} \tag{12}$$

where λ_m's are the eigenvalues of the product matrix $\mathbf{R}^{t*}\mathbf{R}_{du}$. Some numerical algorithms may be used to obtain the eigenvalues. The probability density function (pdf) of D and $p(D)$ can be calculated as an inverse Laplace transform of $\varphi(s)$ using the eigenvalues. The probabilities that $D \geq 0$ and $D < 0$ can then be calculated using the pdf.

Note that if the eigenvalues are distinct, (12) may be rewitten as [10]

$$\varphi(s) = \sum_{m=1}^{6} \frac{A_m}{1+s\lambda_m} \tag{13}$$

where A_m's are the residues of $\varphi(s)$. In this case, the probability of $D \geq 0$ can be calculated as

$$\text{Prob}\{D \geq 0\} = \sum_{\substack{m=1 \\ \lambda_m \geq 0}}^{6} A_m. \tag{14}$$

B. Multiframe Observation

In the case of $K > 1$, an additional index l is used to express the lth unique word, where vector $\mathbf{z}$, given by (6.2), is rewitten as

$$\mathbf{z}_l = [\mathbf{z}_{mdl}^{\langle 1\rangle}\, \mathbf{z}_{mul}^{\langle 1\rangle}\, \mathbf{z}_{mdl}^{\langle 2\rangle}\, \mathbf{z}_{mul}^{\langle 2\rangle}\, \mathbf{z}_{mnl}^{(1)}\, \mathbf{z}_{mnl}^{(2)}] \tag{15}$$

where $\mathbf{z}_{mdl}^{\langle i\rangle}$ and $\mathbf{z}_{mul}^{\langle i\rangle}$ are, with $i = 1 \cdots 2$, the ith path components of the desired signal and interference, respectively, in the matched filter output at the lth unique word timing. $\mathbf{z}_{mnl}^{(i)}$ is the noise component in the ith element output. Using $\mathbf{z}_l$, the decision variable given by (4) can also be expressed in a quadratic form as

$$D = \tfrac{1}{2}\hat{\mathbf{z}}^{t*}\hat{\mathbf{R}}\hat{\mathbf{z}} \tag{16.1}$$

$$\mathbf{R}_{11} = \begin{bmatrix} |\alpha_{11}^{\langle 1\rangle}|^2 - |\alpha_{21}^{\langle 1\rangle}|^2 & \alpha_{11}^{\langle 1\rangle}\alpha_{12}^{\langle 1\rangle *} - \alpha_{21}^{\langle 1\rangle}\alpha_{22}^{\langle 1\rangle *} & \alpha_{11}^{\langle 1\rangle}\alpha_{12}^{\langle 2\rangle *} - \alpha_{21}^{\langle 1\rangle}\alpha_{22}^{\langle 2\rangle *} & \alpha_{11}^{\langle 1\rangle}\alpha_{11}^{\langle 2\rangle *} - \alpha_{21}^{\langle 1\rangle}\alpha_{21}^{\langle 2\rangle *} \\ \alpha_{11}^{\langle 1\rangle *}\alpha_{12}^{\langle 1\rangle} - \alpha_{21}^{\langle 1\rangle *}\alpha_{22}^{\langle 1\rangle} & |\alpha_{12}^{\langle 1\rangle}|^2 - |\alpha_{22}^{\langle 1\rangle}|^2 & \alpha_{12}^{\langle 1\rangle}\alpha_{12}^{\langle 2\rangle *} - \alpha_{22}^{\langle 1\rangle}\alpha_{22}^{\langle 2\rangle *} & \alpha_{12}^{\langle 1\rangle}\alpha_{11}^{\langle 2\rangle *} - \alpha_{22}^{\langle 1\rangle}\alpha_{21}^{\langle 2\rangle *} \\ \alpha_{11}^{\langle 1\rangle *}\alpha_{12}^{\langle 2\rangle} - \alpha_{21}^{\langle 1\rangle *}\alpha_{22}^{\langle 2\rangle} & \alpha_{12}^{\langle 1\rangle *}\alpha_{12}^{\langle 2\rangle} - \alpha_{22}^{\langle 1\rangle *}\alpha_{22}^{\langle 2\rangle} & |\alpha_{21}^{\langle 2\rangle}|^2 - |\alpha_{22}^{\langle 2\rangle}|^2 & \alpha_{12}^{\langle 2\rangle}\alpha_{11}^{\langle 2\rangle *} - \alpha_{22}^{\langle 2\rangle}\alpha_{21}^{\langle 2\rangle *} \\ \alpha_{11}^{\langle 1\rangle *}\alpha_{11}^{\langle 2\rangle} - \alpha_{21}^{\langle 1\rangle *}\alpha_{21}^{\langle 2\rangle} & \alpha_{12}^{\langle 1\rangle *}\alpha_{11}^{\langle 2\rangle} - \alpha_{22}^{\langle 1\rangle *}\alpha_{21}^{\langle 2\rangle} & \alpha_{12}^{\langle 2\rangle *}\alpha_{11}^{\langle 2\rangle} - \alpha_{22}^{\langle 2\rangle *}\alpha_{21}^{\langle 2\rangle} & |\alpha_{11}^{\langle 2\rangle}|^2 - |\alpha_{21}^{\langle 2\rangle}|^2 \end{bmatrix} \tag{6.4}$$

$$\mathbf{R}_{12} = \begin{bmatrix} \alpha_{11}^{\langle 1\rangle} & \alpha_{12}^{\langle 1\rangle} & \alpha_{11}^{\langle 2\rangle} & \alpha_{12}^{\langle 2\rangle} \\ -\alpha_{21}^{\langle 1\rangle} & -\alpha_{22}^{\langle 1\rangle} & -\alpha_{21}^{\langle 2\rangle} & -\alpha_{22}^{\langle 2\rangle} \end{bmatrix}^t \tag{6.5}$$

and

$$\mathbf{R}_{22} = \begin{bmatrix} 1 & 0 \\ 0 & -1 \end{bmatrix}. \tag{6.6}$$

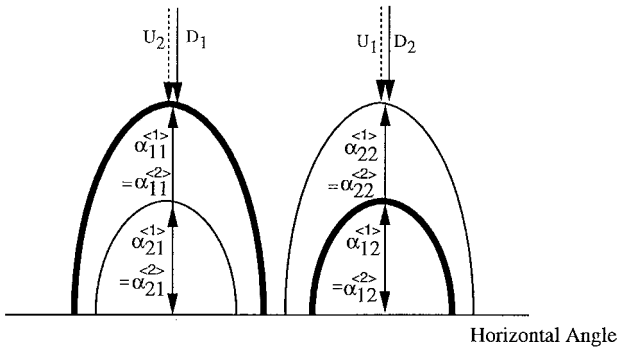

Fig. 4. Propagation scenario for numerical calculations.

where

$$\hat{\mathbf{z}} = [\mathbf{z}_1 \quad \mathbf{z}_2 \quad \cdots \quad \mathbf{z}_M] \tag{16.2}$$

and

$$\hat{\mathbf{R}} = \begin{bmatrix} \mathbf{R} & 0 & \cdots & 0 \\ 0 & \mathbf{R} & & \vdots \\ \vdots & & \ddots & 0 \\ 0 & \cdots & 0 & \mathbf{R} \end{bmatrix}. \tag{16.3}$$

The pdf of D can be obtained through the characteristic function approach by using $\hat{\mathbf{R}}$ and $\hat{\mathbf{z}}$'s autocorrelation matrix $\hat{\mathbf{R}}_{du} = \langle \hat{\mathbf{z}}^{t*} \hat{\mathbf{z}} \rangle$ instead of $\mathbf{R}$ and $\mathbf{R}_{du}$ in (10), respectively, where the size of $\hat{\mathbf{R}}_{du}$ becomes $6K \times 6K$.

IV. Numerical Calculations

Fig. 4 shows the model used in numerical calculations. It is assumed that the desired user's first path has the same incoming direction as the interferer's second path (in this case, $\alpha_{11}^{\langle 1 \rangle} = \alpha_{11}^{\langle 2 \rangle}$ and $\alpha_{21}^{\langle 1 \rangle} = \alpha_{21}^{\langle 2 \rangle}$), and the desired user's second path has the same incoming direction as the interferer's first path ($\alpha_{22}^{\langle 1 \rangle} = \alpha_{22}^{\langle 2 \rangle}$ and $\alpha_{12}^{\langle 1 \rangle} = \alpha_{12}^{\langle 2 \rangle}$). Furthermore, we assume for simplicity

$$\alpha_{11}^{\langle 1 \rangle} = \alpha_{22}^{\langle 1 \rangle} = \alpha_{11}^{\langle 2 \rangle} = \alpha_{22}^{\langle 2 \rangle} = g \exp(-j\theta_m) \tag{17.1}$$

and

$$\alpha_{12}^{\langle 1 \rangle} = \alpha_{21}^{\langle 1 \rangle} = \alpha_{12}^{\langle 2 \rangle} = \alpha_{21}^{\langle 2 \rangle} = g\delta \exp(-j\theta_s) \tag{17.2}$$

where $g \exp(-j\theta_m)$ is the main beam's complex gain and $g\delta \exp(-j\theta_s)$ is the sidelobe beam's complex gain. g is the main beam's amplitude gain, and δ is the sidelobe attenuation factor.

QPSK is assumed for a modulation scheme. Unique word length L and frame length are, respectively, assumed to be 4 and 256 symbol long. The desired user transmits a fixed quaternary unique word pattern at every unique word timing, and the interferer transmits a quaternary random sequence, but the interferer's symbol timing is not synchronized with the desired user's. A Nyquist raised cosine transfer function was used for an overall filter response that is shared equally by the transmitter and receiver. The overall filter response waveform $h(t)$ is given by

$$h(t) = \frac{\sin\left(\frac{\pi t}{T_s}\right)}{\frac{\pi t}{T_s}} \frac{\cos\left(\frac{a\pi t}{T_s}\right)}{1 - \left(\frac{2at}{T_s}\right)^2} \tag{18}$$

where a is the rolloff factor. This waveform is equivalent to the autocorrelation function $\phi(\tau)$ of the noise component at the receiver filter output.

Prior to the PIBS calculations, the effects of timing offset ΔT, per-symbol sampling times M, and the power ratio of the two interference components, U_1/U_2, were evaluated. It was found from the preliminary calculations that the PIBS is insensitive to these factors, and, therefore, in the following PIBS calculations, $M = 1$ and $U_1/U_2 = 0$ dB were assumed. For a fixed desired signal's unique word pattern, PIBS was calculated for various interference waveforms corresponding to the random symbol patterns having symbol timing difference ΔT from the desired signal and then averaged. This process was repeated for other unique word patterns and further averaged. It is assumed that $g^2 = 10$ dB, $\delta^2 = -10$ dB, $\theta_m = 0$, $\theta_s = \pi$, and $a = 0.5$.

A. Power-Limited Environment

In power-limited environments, $U_1 \to 0$ and $U_2 \to 0$. The average SNR Γ on the omnidirectional antenna becomes $\Gamma = (D_1 + D_2)/N$. Fig. 5 shows, for the averaging times $K = 4$, the average Prob$(D < 0)$ versus the average SNR Γ on the omnidirectional antenna, with the power ratio D_1/D_2 and the desired signal's maximum Doppler frequency $f_{Dd}T_s$ normalized by the symbol duration T as parameters. The average Prob$(D < 0)$ decreases as the average SNR increases. This decrease in Prob$(D < 0)$ is more rapid with $f_{Dd}T_s = 0.01$ than with $f_{Dd}T_s \to 0$. This is because of the time–diversity improvement inherent within the averaging process. As the average SNR becomes large, the decrease in Prob$(D < 0)$ plateaus. This floor in Prob$(D < 0)$ is due to D_1/D_2; even for a sufficiently large value of Γ, a beam receiving the desired signal component on the second path is likely to be selected if the second path component has a large signal power.

$$\mathbf{R}_{du} = \langle \mathbf{z}^{t*} \mathbf{z} \rangle = \begin{bmatrix} \mathbf{r}_{ss}^{t*} \mathbf{R}_d^{\langle 1 \rangle} \mathbf{r}_{ss} & 0 & \cdots & 0 \\ 0 & \mathbf{r}_{su}^{t*} \mathbf{R}_u^{\langle 1 \rangle} \mathbf{r}_{su} & & \\ & & \mathbf{r}_{ss}^{t*} \mathbf{R}_d^{\langle 2 \rangle} \mathbf{r}_{ss} & \vdots \\ \vdots & & & \mathbf{r}_{su}^{t*} \mathbf{R}_u^{\langle 2 \rangle} \mathbf{r}_{su} \\ & & & \mathbf{r}_s^{t*} \mathbf{R}_n \mathbf{r}_s \quad 0 \\ 0 & & \cdots & 0 \quad \mathbf{r}_s^{t*} \mathbf{R}_n \mathbf{r}_s \end{bmatrix}. \tag{11}$$

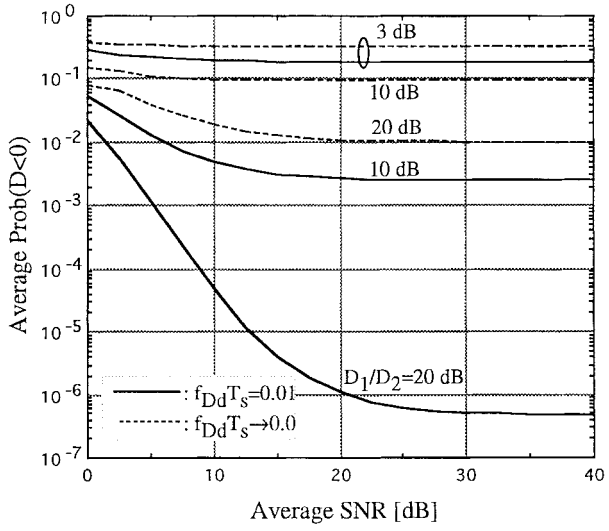

Fig. 5. Average Prob$(D < 0)$ under power-limited environment.

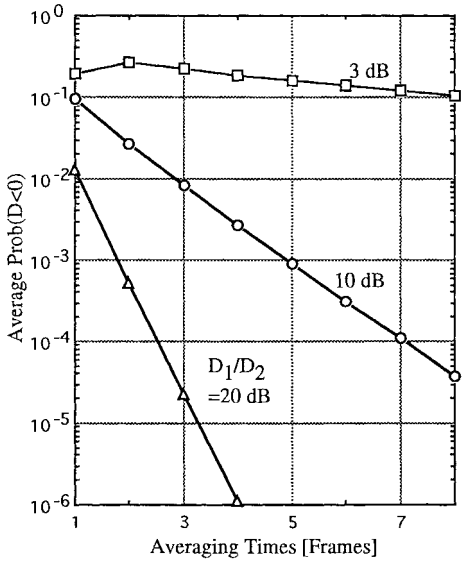

Fig. 6. Average Prob$(D < 0)$ versus number of unique words for averaging under a power-limited environment.

Fig. 6 shows, for the average SNR $\Gamma = 20$ dB and $f_{Dd}T_s = 0.01$, the average Prob $(D < 0)$ versus the number M of the unique words for averaging, with D_1/D_2 as a parameter. The time–diversity improvement achieved by the averaging process can be seen clearly in the plot of the average Prob $(D < 0)$. However, for $D_1/D_2 = 3$ dB, the decrease in the average Prob $(D < 0)$ is very slow, and, hence, averaging is not effective.

B. Interference-Limited Environment

In interference-limited environments, $N \to 0$. The average SIR power ratio Λ on the omnidirectional antenna becomes $\Lambda = (D_1 + D_2)/(U_1 + U_2)$. Fig. 7 shows, for $K = 4$, the average Prob $(D < 0)$ versus the average SIR Λ on the omnidirectional antenna, with D_1/D_2 and the desired and interference signals' normalized maximum Doppler frequency $f_{Dd}T_s = f_{Du}T_s$ as parameters. The similarlity to the average Prob $(D < 0)$ in the power-limited environment can be seen in the performance in the interference-limited environment. The time–diversity improvement can be obtained if D_1/D_2 is large and $f_{Dd}T_s = f_{Du}T_s > 0$.

The average Prob$(D < 0)$ versus D_1/D_2 is shown in Fig. 8 for $K = 4$ and $\Lambda = 20$ dB, with $f_{Dd}T_s = f_{Du}T_s$ as a parameter. As D_1/D_2 increases, the average Prob $(D < 0)$ reduces. If $f_{Dd}T_s = f_{Du}T_s = 0.01$, this Prob $(D < 0)$ reduction is in proportion to $(D_1/D_2)^{-4}$. This indicates that the equivalent diversity order of four can be achieved with $K = 4$. This is because with the frame length of 256 symbols, the fading variations at the four unique word timings are statistically independent for $f_{Dd}T_s = f_{Du}T_s = 0.01$. If fading is very slow ($f_{Dd}T_s = f_{Du}T_s \to 0$), no time–diversity improvement is achieved; the Prob $(D < 0)$ reduction is in proportion to $(D_1/D_2)^{-1}$.

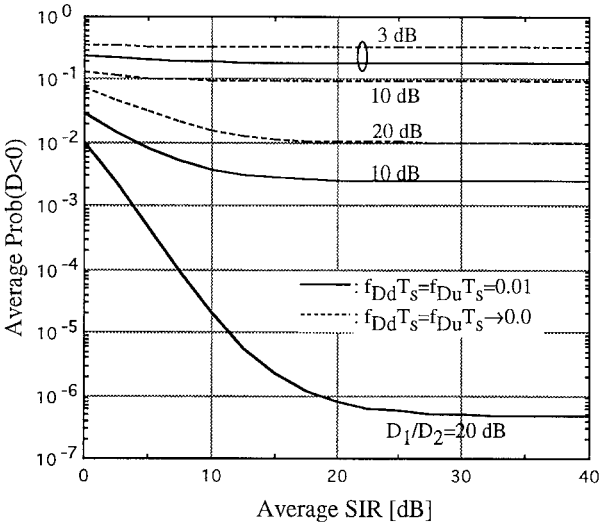

Fig. 7. Average Prob$(D < 0)$ under interference-limited environment.

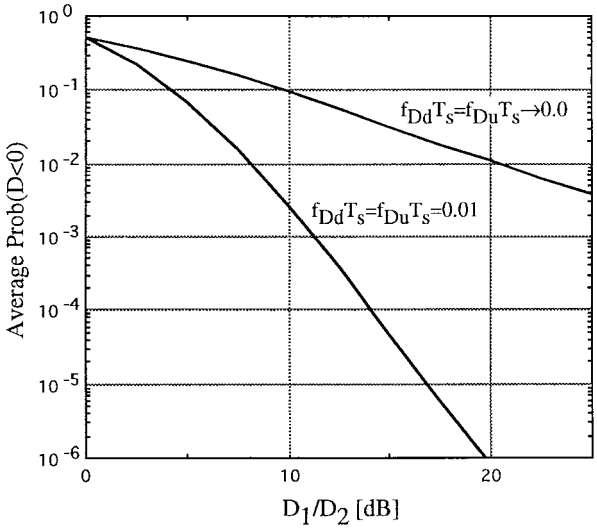

Interference Limited Environment (Γ→∞)
QPSK
Frame Length = 256 Symbol
Unique Word = 4 Symbols
Averaging over 4 Unique Words
1 Sample/Symbol
Timing Offset ΔT=0
Average SIR Λ=20.0 dB
U_1/U_2 = 0 dB

Fig. 8. Average Prob$(D < 0)$ versus D_1/D_2.

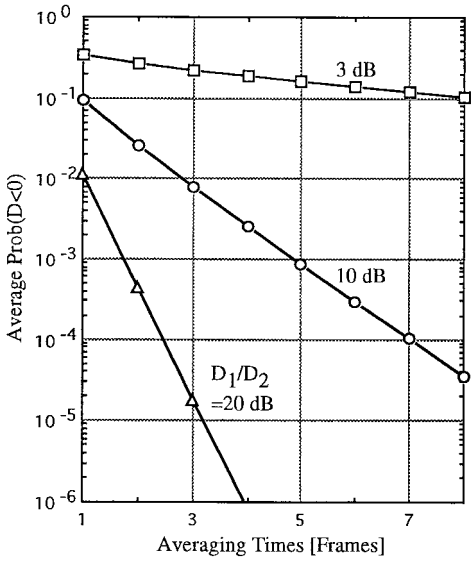

Interference Limited Environment (Γ→∞)
QPSK
Frame Length = 256 Symbol
Unique Word = 4 Symbols
1 Sample/Symbol
Timing Offset ΔT=0
Average SIR Λ=20 dB
U_1/U_2=0.0 dB
$f_{Dd}T_s$=$f_{Du}T_s$=0.01

Fig. 9. Average Prob$(D < 0)$ versus number of unique words for averaging under interference-limited environment.

Fig. 9 shows, for $\Lambda = 20$ dB and $f_{Dd}T_s = f_{Du}T_s = 0.01$, the average Prob $(D < 0)$ versus the averaging times K, with D_1/D_2 as a parameter. The time–diversity improvement achieved by the averaging process can clearly be seen in the plot of the average Prob $(D < 0)$; however, for a small value of D_1/D_2, averaging is not effective.

V. Discussions

Let us assume that fading envelope variations with the desired and interference signal components received by the selected beam are independent of the beam-selection process. This assumption is not always correct. However, if the frame length is sufficiently large compared to the maximum Doppler frequency, this assumption is a reasonable approximation. In this section, impacts of the incorrect beam selection on the average overall SNR and SIR are investigated.

A. Power-Limited Environment

Average SNR's on the first and second element outputs are $\Gamma_1 = (g^2 D_1 + g^2\delta^2 D_2)/N$ and $\Gamma_2 = (g^2\delta^2 D_1 + g^2 D_2)/N$, respectively. If $\Gamma_2 \leq \Gamma_1$, the first element has the correct main beam. This condition is equivalent to $\kappa \geq 1$, where $\kappa = D_1/D_2$. Hence, *average* PIBS = *average* Prob $(D < 0)$ if $\kappa \geq 1$. For the average PIBS of P_b, the average overall SNR Γ_0 after beam selection can be approximated by

$$\Gamma_0 = \Gamma_1(1 - P_b) + \Gamma_2 P_b. \tag{19}$$

The gain Γ_0/Γ in the average overall SNR Γ_0 over the omnidirectional antenna's average SNR Γ then becomes

$$\frac{\Gamma_0}{\Gamma} = \frac{(1 - P_b)g^2(\kappa + \delta^2) + P_b g^2(\kappa\delta^2 + 1)}{\kappa + 1}. \tag{20}$$

Fig. 10 shows the gain Γ_0/Γ in the average SNR versus $\kappa = D_1/D_2$, with the average PIBS as a parameter for $g^2 = 10$ dB and $\delta^2 = -10$ dB. Γ_1/Γ and Γ_2/Γ are also plotted. It is found that the gain on the correct beam increases, and the gain on the incorrect beam decreases as D_1/D_2 increases. The gain on the correct beam approaches its maximum of $g^2 = 10$ dB. The gain on the incorrect beam approaches its minimum of 0 dB. Even with PIBS $= 0.5$, the gain is around 7.3 dB for all the values of D_1/D_2. With PIBS < 0.5, the gain is between 7.3 dB and the gain on the correct beam. Hence, in power-limited environments, an SNR improvement of over 7.3 dB can be achieved with $g^2 = 10$ dB and $\delta^2 = -10$ dB, even if the average PIBS is relatively large.

B. Interference-Limited Environment

SIR's on the first and second element output are $\Lambda_1 = (D_1 + \delta^2 D_2)/(\delta^2 U_1 + U_2)$ and $\Lambda_2 = (\delta^2 D_1 + D_2)/(U_1 + \delta^2 U_2)$, respectively. If $\Lambda_2 \leq \Lambda_1$, the first element has the correct main beam. This condition is equivalent to $\kappa\nu \geq 1$, where $\kappa = D_1/D_2$ and $\nu = U_1/U_2$. Hence, *average* PIBS = *average* Prob $(D < 0)$ if $\kappa\nu \geq 1$. The average overall SIR Λ_0 after beam selection can be approximated by

$$\Lambda_0 = \Lambda_1(1 - P_b) + \Lambda_2 P_b. \tag{21}$$

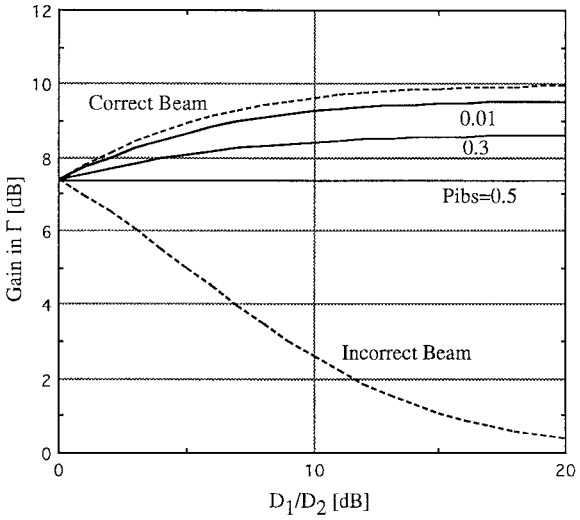

Power Limited Environment (Λ→∞)
Main Beam Gain=10 dB
Sidelobe Attenuation = 10 dB

Fig. 10. Gain in average SNR (dB) under power-limited environment.

The gain Λ_0/Λ in the average overall SIR Λ_0 over the omnidirectional antenna's average SIR Λ then becomes

$$\frac{\Lambda_0}{\Lambda} = \frac{\{1-(1-\delta^2)P_b\}\kappa + \{P_b+(1-P_b)\delta^2\}}{\{P_b+(1-P_b)\delta^2\}\nu + \{1-(1-\delta^2)P_b\}} \cdot \frac{\nu+1}{\kappa+1}. \tag{22}$$

Fig. 11(a) and (b) shows the gain Λ_0/Λ in the average SIR versus $\kappa = D_1/D_2$, with the average PIBS as a parameter for $g^2 = 10$ dB and $\delta^2 = -10$ dB. Fig. 11(a) is for $U_1/U_2 \to \infty$, and Fig. 11(b) is for $U_1/U_2 = 0$ dB. Λ_1/Λ and Λ_2/Λ are also plotted versus κ. It is found that the gain on the correct beam increases, and the gain on the incorrect beam decreases as D_1/D_2 increases. The gain on the correct beam approaches its maximum of $g^2 = 10$ dB. The gain on the incorrect beam approaches its minimum of 0 dB. It is obvious that if PIBS $= 0.5$, the gain is 0 dB. With PIBS < 0.5, a positive gain can be achieved for both cases of $U_1/U_2 \to \infty$ and $U_1/U_2 = 0$ dB, and the gain for $U_1/U_2 \to \infty$ is larger than for $U_1/U_2 = 0$ dB. Hence, an SIR improvement can also be achieved in interference-limited environments, even if the average PIBS is relatively large.

VI. Conclusion

In this paper, we have analyzed the PIBS with a switched multibeam antenna system under power-limited and interference-limited mobile communication environments. A simple beam-selection mechanism was assumed; complex correlation peaks corresponding to the unique words, detected by the matched filter matched to the unique word waveform, are averaged over several consecutive unique words, and a beam having the largest output is then selected. Noncoherent integration was assumed for the averaging process. The beam selection takes place frame-by-frame.

A two-beam antenna was assumed. It was assumed that there is one desired user and one interferer and that each of the desired and interference transmissions has two propagation paths: one goes to one of the two beams, and the other goes to the other beam. With this model, the decision variable asso-

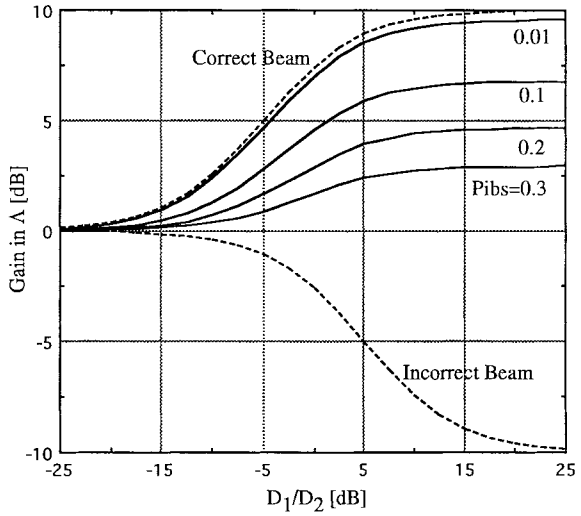

Interference Limited
Environment (Γ→∞)
U1/U2→∞
Main Beam Gain=10 dB
Sidelobe Attenuation = 10 dB

(A) U1/U2→∞

(a)

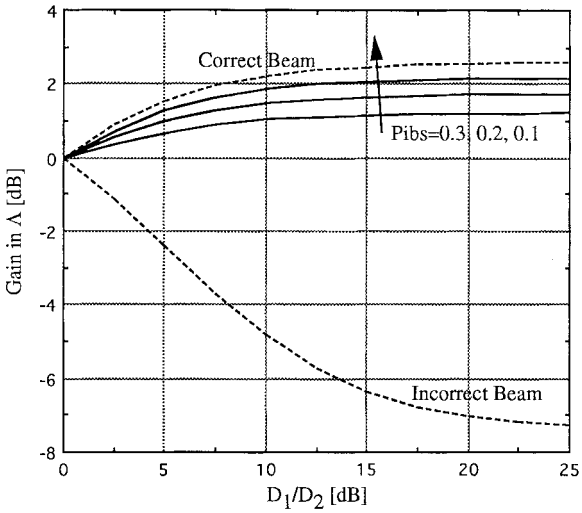

Interference Limited
Environment (Γ→∞)
U1/U2→0 dB
Main Beam Gain=10 dB
Sidelobe Attenuation = 10 dB

(B) U1/U2→0 dB

(b)

Fig. 11. (a) Gain in average SIR versus D_1/D_2 under interference-limited environment for $U_1/U_2 \to \infty$ and (b) gain in average SIR versus D_1/D_2 under interference-limited environment for $U_1/U_2 = 0$ dB.

ciated with the PIBS turns out to be expressed as a quadratic form of the complex random variable vector comprised of desired interference and noise components at the matched filter outputs. Hence, the characteristic function approach has been used to derive the pdf of the decision variable.

It has been shown that the PIBS is dominated by the power ratio D_1/D_2 of the two desired signal components; if the ratio is small, a relatively high PIBS results. The averaging process itself is not effective to reduce the PIBS if D_1/D_2 is small. Time–diversity improvements can be achieved on the PIBS versus D_1/D_2 by the averaging process if the maximum Doppler frequency is relatively high compared with the frame length.

The impacts of the incorrect beam selection on overall average SNR and SIR were then investigated, both in the power-limited and interference-limited environments. Under the power-limited environment, the overall SNR improvement over the omnidirectional antenna is relatively large, even with PIBS ≈ 0.5. Under the interference-limited environment, larger overall SIR improvement can be achieved by smaller PIBS and larger D_1/D_2 values if the interferer has only one propagation path ($U_1/U_2 \rightarrow \infty$). If $U_1/U_2 = 0$ dB, the impact of the beam selection on the overall SIR improvement is small. It should be emphasized that the receiver must tolerate such an SNR (or SIR) encountered by the incorrect beam, even if the PIBS (and, hence, the time during which the incorrect beam is selected) can be made very small.

ACKNOWLEDGMENT

The authors would like to thank Prof. A. Paulraj of Stanford University and K. Kaczmarek, former Vice President of Nextel Communications, for their helpful comments and suggestions. The authors also would like to thank Dr. A. Chatterjee, former Director of Nextel Communications, for his helpful advice on manuscript improvement.

REFERENCES

[1] S. C. Swales, M. A. Beach, D. J. Edwards, and J. P. McGeehan, "The performance enhancement of multibeam adaptive base-station antennas for cellular land mobile radio systems," *IEEE Trans. Veh. Technol.*, vol. 39, pp. 56–67, Feb. 1990.

[2] S. C. Swales, M. A. Beach, and D. J. Edwards, "Multi-beam adaptive base-station antennas for cellular land mobile radio systems," in *Proc. IEEE VTC '89*, San Francisco, CA, 1989, pp. 341–348.

[3] A. F. Naguib, A. Paulraj, and T. Kailath, "Capacity improvement with base-station antenna arrays in cellular CDMA," *IEEE Trans. Veh. Technol.*, vol. 43, pp. 691–698, Aug. 1994.

[4] J. H. Winters, "Optimum combining in digital mobile radio with co-channel interference," *IEEE Trans. Veh. Technol.*, vol. VT-33, pp. 144–155, Aug. 1984.

[5] R. G. Vaughan, "On optimum combining at the mobile," *IEEE Trans. Veh. Technol.*, vol. 37, pp. 181–188, Nov. 1988.

[6] J. H. Winters, "Signal acquisition and tracking with adaptive arrays in the digital mobile radio system IS-54 with flat fading," *IEEE Trans. Veh. Technol.*, vol. 42, pp. 37–384, Nov. 1993.

[7] ——, "The impact of antenna diversity on the capacity of wireless communications systems," *IEEE Trans. Commun.*, vol. 42, pp. 1740–1751, Feb./Mar./Apr. 1994.

[8] R. A. Shade and A. M. Kowalski, "Intelligent antennas for cellular communications," in *Proc. IEEE 1994 Adaptive Ant. Syst. Symp.*, pp. 29–36.

[9] W. C. Jakes, *Microwave Mobile Communications.* New York: IEEE Press, 1974, pp. 19–26.

[10] M. Schwarz, W. Bennett, and S. Stein, *Communications Systems and Techniques.* New York: McGraw-Hill, 1966, pp. 468–480.

[11] A. Mehrotra, *Cellular Radio-Analog and Digital Systems.* Norwood, MA: Artech House, 1994, pp. 54–55.

Tadashi Matsumoto (M'84–SM'95) received the B.S., M.S., and Ph.D. degrees in electrical engineering from Keio University, Yokohama-shi, Japan, in 1978, 1980, and 1991, respectively.

In April 1980, he joined Nippon Telegraph and Telephone Corporation (NTT). From April 1980 to May 1987, he researched signal transmission technologies, such as modulation/demodulation schemes, as well as radio link design for mobile communications systems. He participated in the R&D project of NTT's high-capacity mobile communications system, where he was responsible for the development of the base-station transmitter/receiver equipment for the system. From May 1987 to February 1991, he researched error-control strategies such as forward error correction (FEC), trellis-coded modulation (TCM), and automatic repeat request (ARQ) in digital mobile radio channels. He developed an efficient new ARQ scheme suitable to the error occurrence in TDMA mobile signal transmission environments. He was involved in the development of a Japanese TDMA digital cellular mobile communications system. He took the leadership for the development of the facsimile and data communications service units for the system. In July 1992, he transferred to NTT Mobile Communications Network, Inc. (NTT DoCoMo), Lafayette, CA. From February 1991 to April 1994, he was responsible for research on CDMA mobile communications systems. He intensively researched multiuser detection schemes for multipath mobile communications environments. He was also responsible for research on error-control schemes for CDMA mobile communications systems. He concentrated on research of a maximum *a posteriori* probability (MAP) algorithm and its reduced complexity version for decoding of concatenated codes. He took the leadership for the development of error-control equipment for NTT DoCoMo's CDMA mobile communications system. From 1992 to 1994, he served as a part-time Lecturer at Keio University. In April 1994, he moved to NTT America and served as a Senior Technical Advisor of a joint project with NTT and NEXTEL Communications. In March 1996, he returned to NTT DoCoMo. Since then, he has been an Executive Research Engineer of DoCoMo's R&D Department.

Dr. Matsumoto is a member of the Institute of Electronics, Information, and Communication Engineers of Japan.

Seiji Nishioka (M'95) received the B.S. degree in electrical engineering from Waseda University, Tokyo, Japan, in 1987.

In April 1987, he joined Nippon Telegraph and Telephone Corporation (NTT). Since then, he has been engaged in the development of mobile radio communication systems. From April 1987 to February 1990, he was involved in the development of NTT's high-capacity mobile communications system. He was mainly involved in the development of a channel resource management method for base stations. He also participated in the trial test of that system. In July 1992, he transferred to NTT Mobile Communications Network, Inc. (NTT DoCoMo), Lafayette, CA. From February 1990 to April 1994, he was involved in the development of a Japanese TDMA digital cellular mobile communications system. He was mainly involved in the development of operations and maintenance equipment for that system. In April 1994, he was transferred to NTT America. From April 1994 to March 1996, he was involved in a joint project with NTT and NEXTEL as a Technical Advisor. He has been mainly involved in two activities in the joint project: audio transmission quality and RF distribution technique. Currently, he is a Senior Manager of NTT America.

Mr. Nishioka is a member of the Institute of Electronics, Information, and Communication Engineers of Japan.

David J. Hodder (S'88–M'90) received the B.S. and M.S. degrees in electrical engineering from the University of Nevada, Reno, in 1990 and 1993, respectively.

Prior to his school years, he spent 16 years with the United States Navy in areas of communication and radar systems. From 1989 to 1994, he was a Chief Radio Engineer at the University of Nevada. In 1991, he joined Telesis Technologies Laboratory, PacTel Corporation, as a Senior RF Engineer for PCS research. From 1994 to 1995, he was a Corporate Manager of RF technology for Nextel Communications. He was a Project Director for the development of a successful switched-beam smart antenna system for a digital enhanced specialized mobile radio (ESMR) system. In 1995, he joined the faculty of Truckee Meadows Community College, Reno, NV. Since then, he has been serving as an Associate Professor of Electronics and Computer Technology. Currently, he is also Vice President of Engineering at Telecommunications Group, Inc., Houston, TX. His research interests cover communications systems design deployment and testing, fiber-optics, and radar-guided vehicles.